Surface Science 605 (2011) 1336–1340

Contents lists available at ScienceDirect

Surface Science

journal homepage: www.elsevier.com/ locate/susc

Polarity determination of wurtzite-type crystals using hard x-ray photoelectron diffraction

Jesse R. Williams [a,b,*], Masaaki Kobata [c], Igor Pis [c,d], Eiji Ikenaga [e], Takeharu Sugiyama [e], Keisuke Kobayashi [c], Naoki Ohashi [a,b]

[a] International Center for Materials Nanoarchitectonics (MANA), National Institute for Materials Science (NIMS), 1-1 Namiki, Tsukuba, Ibaraki 305-0044, Japan
[b] NIMS Saint-Gobain Research Center of Excellence for Advanced Materials, NIMS, 1-2-1 Sengen, Tsukuba, Ibaraki 305-0047, Japan
[c] Beamline Station, National Institute for Materials Science (NIMS), SPring-8, 1-1-1, Kouto, Sayo-cho, Sayo-gun, Hyogo 679-5198, Japan
[d] Department of Surface and Plasma Science, Faculty of Mathematics and Physics, Charles University, V Holešovičkách 2, 18000 Prague 8, Czech Republic
[e] Japan Synchrotron Radiation Research Institute (JASRI), 1-1-1, Kouto, Sayo-cho, Sayo-gun, Hyogo 679-5198, Japan

ARTICLE INFO

Article history:
Received 1 December 2010
Accepted 28 April 2011
Available online 5 May 2011

Keywords:
Wurtzite-type crystal
Polarity
Zinc oxide
Photoelectron diffraction

ABSTRACT

The surface structure of a single-crystal ZnO wafer was studied by angle-resolved x-ray photoelectron spectroscopy (ARXPS) using synchrotron radiation. As a result, well-defined x-ray photoelectron diffraction (XPD) patterns were obtained for the (0001) and ($000\bar{1}$) polar surfaces using the photoemission from the Zn $2p_{3/2}$ and O 1s core levels. The XPD patterns were indexed assuming forward scattering of photoelectrons by neighboring ions. Further, the XPD patterns for the (0001) and ($000\bar{1}$) surfaces were different from each other, indicating the possibility for using the XPD technique for polarity determination.
© 2011 Elsevier B.V. All rights reserved.

1. Introduction

Wide-band-gap semiconductors such as zinc oxide (ZnO) and gallium nitride (GaN) have a hexagonal wurtzite-type (WZ-type) crystal structure. Because of this hexagonal structure, epitaxial layers of WZ-type crystals are usually deposited such that their c-axis is parallel to the growth direction [1,2]. Further, WZ-type crystals have polar surfaces. Therefore, the crystalline quality and the microstructure of the epitaxial layers depend on whether they are grown on the (0001) cation-terminated surface or the ($000\bar{1}$) anion-terminated surface [3,4]. Furthermore, WZ-type crystals exhibit spontaneous polarization and piezoelectric effect along the c-axis. Thus, these crystals are useful for the fabrication of electric devices such as microelectromechanical devices [5] and transistors using a two-dimensional electron gas [6]. However, it has been found that the polarization of WZ-type crystals causes reduction of efficiency in light emitting diodes made from nitride semiconductors [7]. Thus, it is important to determine the c-axis polarity of WZ-type crystals.

Currently, polarity determination of WZ-type crystals is carried out by chemical etching [8], convergent beam electron diffraction (CBED) [9], or coaxial impact collision ion scattering spectroscopy (CAICISS) [10]. However, these methods are destructive; etching can cause damage to the surface structure, and CBED requires very thin specimens for electron diffraction using transmission electron microscopy (TEM) with specific settings. Also it is difficult to determine the polarity on polycrystalline thin films using etching because grain boundary etching is very fast, and in this case both polar faces will etch quickly [11]. On the other hand, CAICISS is nondestructive but requires special ion-scattering apparatus and is only useful for samples having a relatively large surface area. Thus, there is a need for new polarity determination techniques that are nondestructive and can be implemented using a conventional setup. Previously, polarity determination has been carried out using scanning nonlinear dielectric microscopy [12] and anomalous dispersion of x-ray diffraction [8]. However, the former can only be used for a localized analysis, both require a reference sample for instrumental calibration, and the latter necessitates prior knowledge of the film thickness. Also, an angular dependent x-ray photoelectron spectroscopy technique has been developed, which utilizes the difference in inelastic mean free path (IMFP) of the Zn $2p_{3/2}$ and O 1s photoelectrons [13]. The measurements were done at polar angles of 0° and 70°; however the azimuth angle and the detector's polar angle acceptance were never stated, so the variation in measured intensity could have been from x-ray photoelectron diffraction (XPD). In fact, there is a neighboring atom at 70.5° in the ($11\bar{2}0$) plane, which means this is a strong diffraction vector. Photoelectron intensity fluctuations due to scattering from neighboring atoms are described later in the discussion section.

To overcome the above drawbacks, in this study, we investigated x-ray photoelectron diffraction (XPD) as a technique for the surface structure analyses, i.e., polarity determination, of WZ-type crystals.

* Corresponding author.
E-mail address: Williams.Jesse@nims.go.jp (J.R. Williams).

0039-6028/$ – see front matter © 2011 Elsevier B.V. All rights reserved.
doi:10.1016/j.susc.2011.04.036

ZnO polar surfaces have previously been studied with XPD, and it has been shown that the diffraction patterns are different for the (0001) and (000$\bar{1}$) surfaces [14,15]. However, in these previous studies, XPD has only been studied in the (10$\bar{1}$0) azimuth plane. We investigate all azimuth angles to determine which polar and azimuth angle result in the strongest variation between the two surfaces to locate the most appropriate angles for polarity determination.

X-ray photoemission spectroscopy (XPS) is characterized by a very high surface sensitivity owing to the very small escape depth of photoelectrons; therefore, it is appropriate for analysis of surface adsorption [14,15], but that also means that unintentional surface adsorption causes serious degradation of the spectral quality. To overcome this drawback of XPS/XPD, we employed hard x-ray radiation (hν = 7939.8 eV) for the present XPS/XPD study, because photoelectrons excited with hard x-rays show a much longer inelastic mean free path than those excited with the conventional soft x-rays such as aluminum Kα (hν = 1486.6 eV). Indeed, Igor et al. [16] successfully observed XPD profiles of a silicon crystal covered with a native oxide layer. As a result, we could successfully demonstrate the polarity determination of a WZ-type crystal, i.e., zinc oxide (ZnO), by employing XPD, as described below.

2. Experiment

A commercially available single crystal ZnO wafer was used as a specimen. The crystal was grown by a hydrothermal method, and the wafer surface was normal to the c-axis of the crystal. The wafer surface was planarized by chemical mechanical polishing (CMP) to obtain a nominal surface roughness of less than 1 nm. Then, the surface polarity of the wafer was determined by chemical etching; with HCl the (000$\bar{1}$) surface etches quickly while the (0001) surface retains its mirror polish [17]. The wafer surface was rinsed with ethanol and acetone before it was introduced into a vacuum chamber for performing angle-resolved XPS (ARXPS) measurements. There were no *in situ* surface cleaning procedures used such as surface sputtering, and hence the O 1s and C 1s peaks due to the adsorbates could be clearly seen if we employed a conventional XPS using an Al Kα x-ray source.

Circularly polarized synchrotron radiation produced with a diamond phase retarder installed at planer undulator beamline BL47XUin SPring-8, Japan, was used for performing the ARXPS measurements. The x-ray energy was fixed at hν = 7939.8 eV, as mentioned above. We investigated the ARXPS spectra by measuring the polar (θ) and azimuth (φ) angle dependencies of the XPS intensity from the Zn $2p_{3/2}$ and O1 s core levels. Using an objective lens with angle resolution capability in conjunction with a VG SCIENTA R4000 10 kV electron energy analyzer (EEA) with an array detector, the θ dependence of the XPS intensity was recorded from 0° to approximately 45° at intervals of 1.18°. More information about the lens and analyzer configuration can be found elsewhere [18]. The φ dependence of the ARXPS intensity profiles was measured by rotating the sample using a goniometer. The φ resolution was about 1°, but measurements were taken at 2° increments. Since the θ-scan profile measured at φ intervals of 60° confirmed that the φ-scan profile showed a six-fold symmetry, we measured the θ dependence of the ARXPS intensity profiles for φ ranging from 0° to 100°. The complete ARXPS intensity pattern (φ = 0°–360°) was produced by applying the six-fold symmetry to the measurement results. It should be noted that the instrumental transmission function, i.e., the θ dependence of the sensitivity of the analyzer, was calibrated using an isotropic sample of amorphous silicon oxide.

3. Results and discussion

The ARXPS intensity patterns of Zn $2p_{3/2}$ and O1 s core levels obtained from the (0001) and (000$\bar{1}$) surfaces of ZnO are shown in

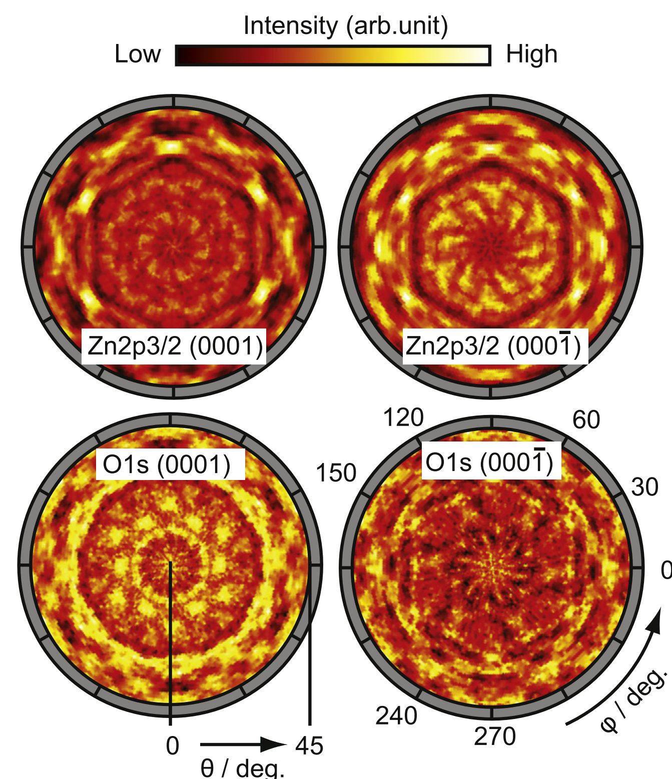

Fig. 1. ARXPS intensity profile for Zn $2p_{3/2}$ and O1 s core levels measured from (0001) and (000$\bar{1}$) surfaces of ZnO. (See text for details.)

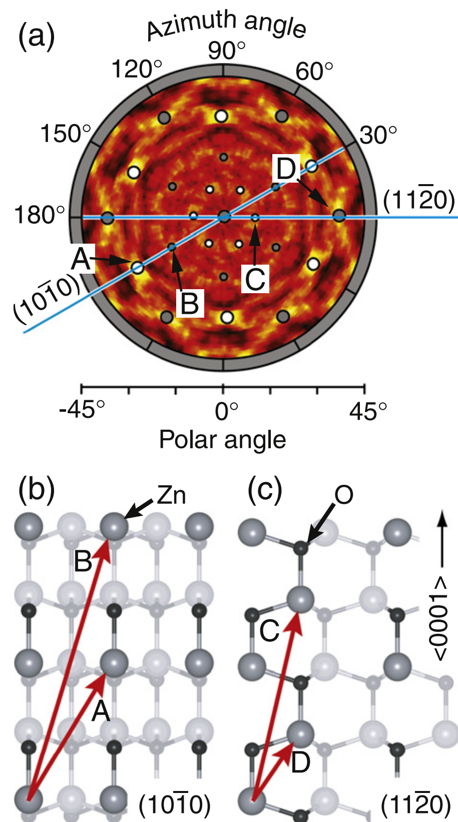

Fig. 2. The intensity maxima of the Zn $2p_{3/2}$ (0001) pattern are indicated in the (10$\bar{1}$0) and (11$\bar{2}$0) planes and the accompanying cross sections of wurtzite crystal are shown. The intensity maxima and vectors in the cross sections are labeled (A, B, C, and D) to illustrate how nearest neighbors position correspond to the measured maxima.

Fig. 1 as pole figure patterns. In this figure, $\varphi=0°$ corresponds to the $(11\bar{2}0)$ plane and $\varphi=30°$ corresponds to the $(10\bar{1}0)$ plane. Because the six-fold symmetry was confirmed for the φ scan, the pattern measured for $\varphi=0°$–$60°$ was reproduced six times to obtain the complete pole figure pattern (360°). As shown in the figure, the four patterns differ from each other, indicating that ARXPS is indeed suitable for polarity determination.

In order to examine the ARXPS intensity variation in Fig. 1 in detail, we analyzed these patterns by assuming that the intensity variation was caused by forward scattering of photoelectrons. Here, we focus on the ARXPS intensity pattern for Zn $2p_{3/2}$ obtained from the (0001) surface. As shown in Fig. 2, a large peak is observed at an angular coordinate of $\varphi=30°$, $\theta\approx32°$(peak A), and other peaks were found at angular coordinates of $\varphi=30°$, $\theta\approx18°$(peak B), $\varphi=0°$, $\theta\approx13°$(peak C), and $\varphi=0°$, $\theta\approx36°$(peak D). Interatomic vectors in Fig. 2 indicate these characteristic angles. For example, the angular coordinate of $\varphi=30°$, $\theta\approx32°$(peak A) corresponds to the vector pointing from a Zn cation to a Zn ion (at a distance of 0.61 nm) on the same $(10\bar{1}0)$ plane, and the angular coordinate of $\varphi=30°$, $\theta\approx18°$(peak B) corresponds to the vector pointing from a Zn cation to a Zn ion (at a distance of 1.09 nm) on the same $(10\bar{1}0)$ plane. Similarly, the angular coordinates of $\varphi=0°$, $\theta\approx13°$(peak C) and $\varphi=0°$, $\theta\approx36°$(peak D) correspond to the vectors pointing from one Zn ion to another Zn ion on the same $(11\bar{2}0)$ plane. Thus, all the obvious peaks found in the ARXPS intensity pattern of Zn $2p_{3/2}$core levels obtained from the (0001) surface can be correlated with interatomic vectors pointing from a Zn ion to its neighboring ions. Although we have not shown similar correlations for the other thee ARXPS patterns, we have confirmed that the peaks found in these ARXPS intensity profiles (Fig. 1) can be correlated with interatomic vectors. In particular, interatomic vectors originating at Zn sites can explain the ARXPS patterns for the Zn $2p_{3/2}$ core level, and interatomic vectors originating at O sites can explain those for the O 1s core level.

The correlation between the ARXPS intensity and the atomic arrangements indicates that the intensity variation is caused by the so-called photoelectron diffraction, namely, forward scattering of photoelectrons by neighboring atoms [16,19]. In this study, the kinetic energies of photoelectrons were 6910 eV for the Zn $2p_{3/2}$ peak and 7401 eV for the O 1s peak. For such high-energy electrons, forward scattering is the dominant scattering process, as indicated by the atomic scattering factor for electrons. In fact, XPD simulations for silicon have shown that strong forward scattering is observed at a kinetic energy of 0.5 keV and that Kikuchi bands originating from the dynamical scattering of electrons from lattice planes are observed if the XPD is excited using hard x-rays [20]. Therefore, indexing the ARXPS profile of ZnO, measured in this study, by assuming forward scattering is quite reasonable, and thus, we may conclude that the ARXPS pattern shown in Fig. 1 can be regarded as an XPD pattern of the ZnO polar surface.

To locate the most appropriate angle for polarity determination, the Zn $2p_{3/2}$ diffraction patterns are analyzed. The diffraction intensity of the $(000\bar{1})$ face is divided by that of the (0001) face in order to find the positions of greatest intensity variation, and the result is shown in the diffraction pattern in Fig. 3. In this two dimensional map the areas of high intensity indicate where there is the greatest difference between patterns; in other words these angles are convenient for

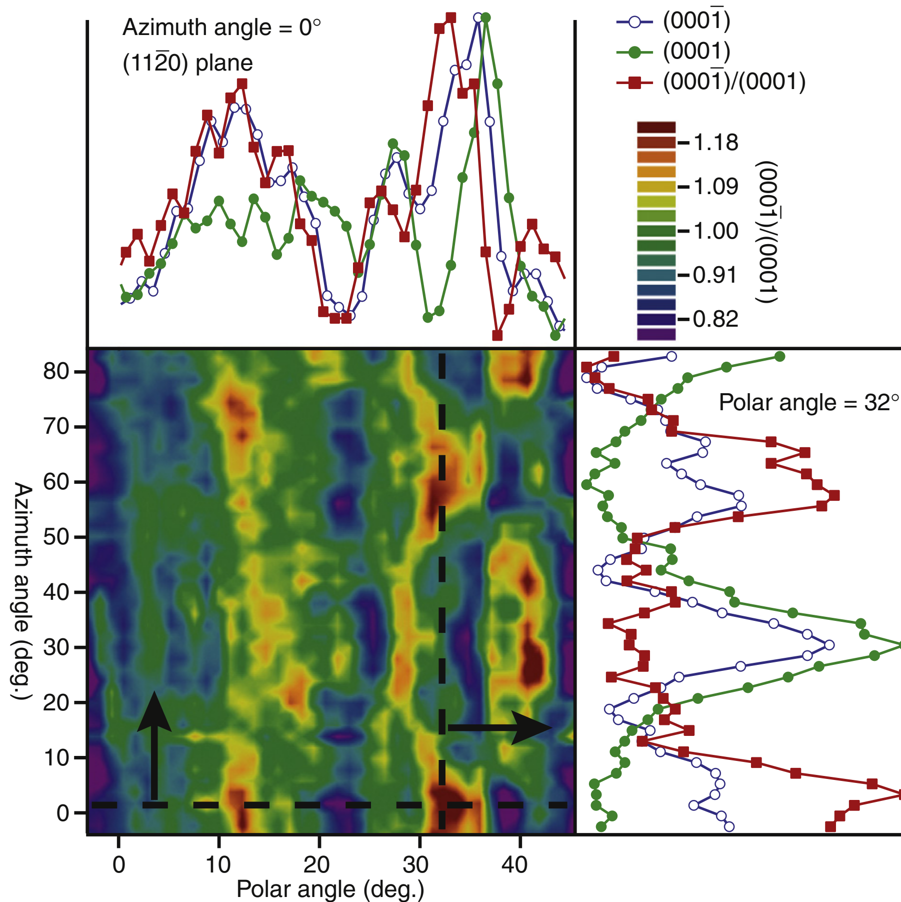

Fig. 3. A two dimensional map of the Zn $2p_{3/2}$ $(000\bar{1})$ intensity divided by the Zn $2p_{3/2}$ (0001) intensity. There are two line scans taken from the map, one at a fixed polar angle 32° and one at a fixed azimuth angle of 0°. In the line scans, the $(000\bar{1})$ surface, (0001) surface, and quotient of the two are represented by open circles, closed circles, and closed squares respectively.

polarity determination. Therefore, performing a φ scan at a characteristic θ angle or a θ scan at a characteristic φ angle is a more efficient way of polarity determination than measuring the complete pole figure pattern for the ARXPS intensity from the (0001) and $(000\bar{1})$ surfaces, as shown in Fig. 1. For example, a φ scan for the Zn $2p_{3/2}$ intensity at $\theta=32°$ can be performed for the efficient determination of polarity using XPD. As seen in Fig. 3, a distinct feature is observed at the angular coordinate of ($\varphi=0°$, $\theta=32°$) and at equivalent coordinates of ($\varphi=60°$, $\theta=32°$) for the Zn $2p_{3/2}$ core level, wherein strong emission is observed for the $(000\bar{1})$ polarity but not for the (0001) polarity. This result indicates that it is not necessary to measure the complete XPD pattern to determine the polarity, but measurements at specific angles are sufficient for this purpose. For the case discussed above, measuring the Zn $2p_{3/2}$ peak intensity at the angular coordinates of ($\varphi=0°$, $\theta=32°$) ($I_{0,32}$) and ($\varphi=30°$, $\theta=32°$) ($I_{30,32}$) to evaluate the $I_{0,32}/I_{30,32}$ ratio is sufficient for polarity determination; $I_{0,32}/I_{30,32}=0.6$ for the (0001) polarity, while $I_{0,32}/I_{30,32}=0.9$ for the $(000\bar{1})$ polarity.

These results clearly show how neighboring atoms influence the angular dependent photoelectron intensity, and hence XPD can explain the result from Zhang et al. [13]. They compare the intensity of the normal emission ($\theta=0°$) to the intensity at $\theta=70°$, but a neighboring atom is found at $\theta=70.5°$ in the $(11\bar{2}0)$ plane. Therefore a significant variation in intensity can be expected from XPD.

We now discuss the reason why polarity determination is possible using XPD. The difference between the (0001) and $(000\bar{1})$ XPD patterns for a given emitter is a result of the relative anion to cation position. If only the Zn cations are considered, then there is no difference between the (0001) and $(000\bar{1})$ configurations. However, the O anions are at different positions with respect to the Zn when in the (0001) and $(000\bar{1})$ configurations. This point is illustrated in Fig. 4,

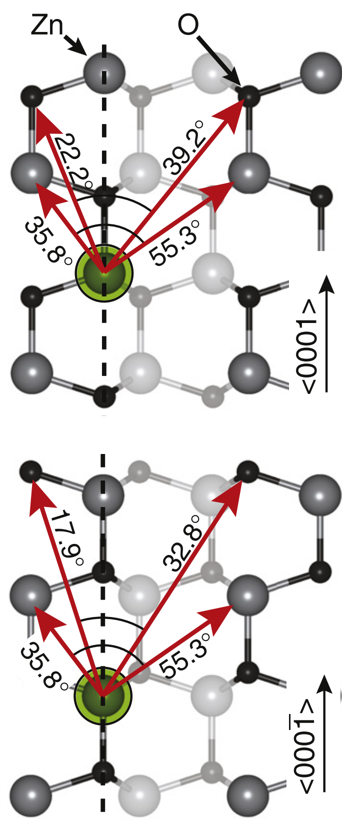

Fig. 4. The wurtzite $(11\bar{2}0)$ plane in the (0001) and $(000\bar{1})$ configuration illustrating the change in cation–anion angles. See the text for a detailed explanation.

which shows the ZnO cross-section in the $(11\bar{2}0)$ plane. Considering a Zn emitter, the angles between other Zn neighbors are the same for the (0001) and $(000\bar{1})$ configurations, but the angles from the Zn emitter to O neighbors differ. This is the origin for the differences seen in the diffraction patterns. For example, in the polar line scan, shown in upper curve of Fig. 3, there is a strong peak at 36° for both polarities, which corresponds to 35.8° Zn–Zn vector indicated in Fig. 4. However, the peak from the $(000\bar{1})$ surface has a shoulder at angles less than 36° (i.e. a shoulder on the left side of the peak), while the peak from the (0001) surface has a shoulder at angles greater than 36° (i.e. a shoulder on the right side of the peak). The difference in peak asymmetry can be explained by the relative positions of O neighbors. In the case of the $(000\bar{1})$ polarity, the Zn emitter has an oxygen neighbor located at 32.8°, and for the (0001) polarity, the relevant O neighbor is located at 39.2°. These O neighbors are responsible for the peak shoulders addressed above.

There are resemblances between the Zn $2p_{3/2}$ intensity profile from the (0001) surface and the O 1s intensity profile from the $(000\bar{1})$ surface (upper left and lower right panels in Fig. 1), and the Zn $2p_{3/2}$ intensity profile from the $(000\bar{1})$ surface and the O 1s intensity profile from the (0001) surface (upper right and lower left panels) because the emitters are in the similar positions with respect to their neighboring atoms. However, there are also differences in the patterns resulting from the emitters' different photoelectron energies, 6910 eV for Zn $2p_{3/2}$ and 7401 eV for O 1s. Furthermore, the scattering factors of the neighboring atoms are also different partially because of the difference in photoelectron energy, but also because the scattering atoms are different in each case.

Finally, we discuss the origin of the six-fold symmetry in the XPD patterns. Because XPD should be sensitive to the atomic arrangements in the topmost layer owing to the short IMFP of photoelectrons, one may expect to observe a three-fold symmetry originating from the *C*3v symmetry of the topmost layer. For the ZnO crystal, the atomic arrangement in the topmost layer is $[OZn_3]$ on the $(000\bar{1})$ surface and $[ZnO_3]$ on the (0001) surface and these layers are aligned to have a three-fold symmetry. However, the φ-scan XPD patterns measured herein show a perfect six-fold symmetry. There are two factors contributing to the origin of the six-fold symmetry: the large IMFP (Λ) resulting from hard x-ray radiation and half steps on the surface. These two factors are discussed below.

Regarding Λ, hard x-ray radiation produces a pattern that is nearly six-fold resulting from the large IMFP (Λ), approximately 10 nm [21]. Because Λ is large compared to the length scale of the unit cell, the intensity variation between each layer is not large. The depth dependent intensity is

$$I = I_0 \ \exp(-d / \Lambda \ \cos\theta) \quad (1)$$

where I_0 is the intensity from an infinitely thick uniform substrate, and d is the depth. The distance from Zn-to-Zn layers or O-to-O layers in the (0001) direction is 0.263 nm, which is d when comparing intensity between layers. When these distances are applied to Eq. (1) in the normal direction, $I=0.97\ I_0$, so there is only a 3% intensity drop from layer to layer. Further illustration for the effect of the IMFP is available in the supporting information [22]. For this reason, the pattern is nearly six-fold in symmetry. Hence the XPD patterns reflect not only the C3v symmetry of the topmost surface but also the translation symmetry of the wurtzite structure, i.e. 6_3 screw axis.

The second factor contributing to the origin of the six-fold symmetry in the surface structure of ZnO has been discussed in the literature conducting a CAICISS study on a ZnO surface [23]; the polished surface of ZnO showed a step-and-terrace structure with a half unit-cell height. Because the aforementioned 6_3 screw axis is included in the symmetry operation of a wurtzite crystal ($P6_3mc$), the presence of the half unit-cell step can be regarded as the cause for the twining of the surface structure. In other words, the presence of

periodically spaced half unit-cell step induces perfect six-fold symmetry in the XPD patterns.

This study has shown that hard x-ray ARXPS offers way to measure the polarity of the wurtzite structure. The most significant advantage of using hard x-ray ARXPS is that it is far less sensitive to surface contamination; as mentioned above our experiments were done without *in situ* surface cleaning, such as sputtering by ion beam. This means that we do not have to be afraid of any ambiguity resulting from the surface preparation. On the other hand, less surface sensitivity is also a major disadvantage of XPD using hard x-ray radiation. While this is good from a contamination perspective, it is not good for measuring diffraction of structural relaxation at the topmost surface or very thin layers of ad-atoms. In such a case, it would be better to use soft x-rays, such as Al Kα radiation. In any energy range of source x-ray, the XPD intensity charts obtained in this study will be an aid for peak identification. This study was done using synchrotron radiation, which is not always easily accessible. However, there are options for laboratory sized hard x-ray sources. For example Cr Kα ($h\nu = 5417.0$ eV) has been used in a laboratory system with ARXPS [18]. Such a system could be used for polarity measurements without the physical limitation of synchrotron radiation.

4. Conclusion

In summary, we measured the ARXPS patterns of a polar ZnO surface, which is a WZ-type wide-band-gap semiconductor, and confirmed that ARXPS produces well-defined XPD patterns because of the forward scattering of photoelectrons. The XPD patterns indicated that the polarity of WZ-type crystals can be determined by selecting specific angles at which the XPS intensities for the (0001) and ($000\bar{1}$) surfaces differ from each other. Hard x-ray radiation was used in this study, and the advantage of hard x-rays was that the measurements were not as surface sensitive as with conventional soft x-rays. Therefore, the measurement could be considered a bulk measurement and was not greatly influenced by surface contamination or relaxation. Theoretical simulations as well as an XPD study using conventional soft x-ray radiation are under progress by the authors, with the aim of establishing XPD as the most conventional method for polarity determination of WZ-type semiconductors.

Acknowledgments

Part of this study was supported by the World Premier International Research Center (WPI) Initiative (MANA/NIMS) of the Ministry for Education, Culture, Sports, Science and Technology (MEXT), Japan; a Grant-in-Aid for Scientific Research (Nos. 19053008 and 20246007) from the Japan Society for Promotion of Science (JSPS); and a grant for the Development of Systems and Technology for Advanced Measurement and Analysis promoted by the Japan Science and Technology Agency (JST), Japan. The synchrotron radiation experiments were performed at BL47XU in SPring-8 with the approval of the Japan Synchrotron Radiation Research Institute (JASRI) as part of the project "Electronic State Analysis of the GRAPHEN by Hard X-ray Photoemission Spectroscopy." I.P. thanks the Czech Grant Agency for a research support (no. GD202/09/H041). Authors also acknowledge helpful discussion with Dr. Hideki Yoshikawa of NIMS.

Appendix A. Supplementary data

Supplementary data to this article can be found online at doi:10.1016/j.susc.2011.04.036.

References

[1] T. Miyata, Y. Minamino, S. Ida, T. Minami, J. Vac. Sci. Technol. A22 (2004) 1711.
[2] P.K. Song, E. Yoshida, Y. Sato, K.H. Kim, Y. Shigesato, Jpn. J. Appl. Phys 43 (2004) L 164.
[3] N. Ohashi, T. Ohgaki, S. Sugimura, K. Maeda, I. Sakaguchi, H. Ryoken, I. Niikura, M. Sato, H. Haneda, Mat. Res. Soc. Symp. Proc. 799 (2003) 255.
[4] H. Xu, K. Ohtani, M. Yamao, H. Ohno, Appl. Phys. Lett. 89 (2006) 071918.
[5] H.P. Lobl, M. Klee, R. Milsom, R. Dekker, C. Metzmacher, W. Brand, P. Lok, J. Euro. Ceram. Soc. 21 (2001) 2633.
[6] A. Tsukazaki, A. Ohtomo, T. Kita, Y. Ohno, H. Ohno, M. Kawasaki, Science 315 (2007) 1388.
[7] H. Masui, A. Chakraborty, B.A. Haskell, U.K. Mishra, J.S. Speck, S. Nakamura, S.P. Denbaars, Jpn. J. Appl. Phys. 44 (2005) L1329 and refs therein.
[8] H. Tampo, P. Fons, A. Yamada, K.K. Kim, H. Shibata, K. Matsubara, S. Niki, H. Yoshikawa, H. Kanie, Appl. Phys. Lett. 87 (2005) 141904.
[9] P.R. Tavernier, T. Margalith, J. Williams, D.S. Green, S. Keller, S.P. DenBaars, U.K. Mishra, S. Nakamuraa, D.R. Clarke, J. Cryst. Growth 264 (2004) 150.
[10] Y. Adachi, N. Ohashi, T. Ohnishi, T. Ohgaki, I. Sakaguchi, H. Haneda, M. Lippmaa, J. Mater. Res 23 (2008) 3269 and refs. therein.
[11] N. Ohashi, K. Takahashi, S. Hishita, I. Sakaguchi, H. Funakubo, H. Haneda, J. Electrochem. Soc. 154 (2007) D82.
[12] S. Kazuta, Y. Cho, H. Odagawa, M. Kadota, Jpn. J. Appl. Phys. 39 (2000) 3121.
[13] L. Zhang, D. Wett, R. Szargan, Surf. Interface Anal. 36 (2004) 1794.
[14] K.H. Ernst, A. Ludviksson, R. Zhang, J. Yoshihara, C.T. Campbell, Phys. Rev. B 47 (1993) 13782.
[15] J. Yoshihara, J.M. Campbell, C.T. Campbell, Sur. Sci. 406 (1998) 235.
[16] I. Píš, M. Kobata, T. Matsushita, H. Nohira, K. Kobayashi, Appl. Phys. Express 3 (2010) 056701.
[17] K. Takahashi, H. Funakubo, N. Ohashi, H. Haneda, Thin Solid Films 486 (2005) 42.
[18] M. Kobata, I. Píš, H. Iwai, H. Yamazui, H. Takahashi, M. Suzuki, H. Matsuda, H. Daimon, K. Kobayashi,Anal. Sci.26 (2010) 227, and Ikenaga et al., unpublished.
[19] S. Kono, C.S. Fadley, N.F.T. Hall, Z. Hussain, Phys. Rev. Lett. 41 (1978) 117.
[20] A. Winkelmann, C.S. Fadley, F.J.G. de Abajo, New J. Phys. 10 (2008) 113002.
[21] C.J. Powell, A. Jablonski, National Institute of Standards and Technology, Gaithersburg, MD, 2010.
[22] See supporting information.
[23] H. Maki, N. Ichinose, S. Sekiguchi, N. Ohashi, T. Nishihara, H. Haneda, J. Tanaka, Jpn. J. Appl. Phys. Part 138 (1999) 2741.